Available online at www.sciencedirect.com
ScienceDirect
Journal of Catalysis 245 (2007) 173–183
JOURNAL OF CATALYSIS
www.elsevier.com/locate/jcat

Enantioselectivity promotion by achiral surface functionalization on SiO_2-supported Cu-bis(oxazoline) catalysts for asymmetric Diels–Alder reactions

Satoka Tanaka, Mizuki Tada, Yasuhiro Iwasawa *

Department of Chemistry, Graduate School of Science, The University of Tokyo, Hongo, Bunkyo-ku, Tokyo, 113-0033, Japan

Received 11 September 2006; revised 4 October 2006; accepted 5 October 2006

Available online 7 November 2006

Abstract

Novel SiO_2-supported chiral Cu-bis(oxazoline) (BOX) complexes for asymmetric Diels–Alder reactions were prepared by combining metal-complex immobilization with surface functionalization using achiral silane-coupling reagents on SiO_2. We found that the surface functionalization of a SiO_2-supported Cu-BOX catalyst with achiral 3-methacryloxypropyltrimethoxysilane dramatically increased enantioselectivity in the asymmetric Diels–Alder reaction of cyclopentadiene and 3-acryloyl-2-oxazolidinone. The Cu-BOX complexes on bare and functionalized SiO_2 surfaces were characterized by XAFS, ESR, FT-IR, UV/vis, and ^{29}Si solid-state MAS NMR. The large increase in enantioselectivity by achiral surface species without chiral center may be due to a glue effect, creating a new chiral ensemble structure at the surface.

Keywords: Asymmetric heterogeneous catalyst; SiO_2-supported Cu-BOX complex; Surface functionalization with achiral organic molecules; Asymmetric Diels–Alder reaction; Amplification of enantioselectivity

1. Introduction

Asymmetric catalysts for fine chemical processes have been developed in homogeneous systems, where precise 3D design of metal organic complexes has been achieved [1–4]. However, there are few examples of heterogeneous asymmetric catalysts, despite the many advantages of these catalysts in industrial processes. Providing asymmetric reaction fields with uniform active sites is generally difficult on solid catalyst surfaces [5]. The simple support of homogeneous asymmetric metal-complex catalysts on solid surfaces brings about large decreases in both catalytic activity and enantioselectivity. A new approach to constructing effective asymmetric reaction environments on surfaces is indispensable for the development of heterogeneous asymmetric catalysts.

Asymmetric Diels–Alder reactions are widely used in pharmaceutics and biosynthesis [6,7]. Cu-bis(oxazoline) (BOX) complex is one of the useful metal complexes for catalyzing asymmetric Diels–Alder reactions [8–16]. There have been several reports on the immobilization of the Cu-BOX complexes on solid surfaces to prepare heterogeneous asymmetric catalysts. The Cu-BOX complexes have been immobilized on laponite, nafion-silica [17], and amorphous silica [18] by electrostatic interactions. They have also been electronically bound on mesoporous and microporous materials [19] and polymers [20,21], and inside the pores of MCM-41 and SBA-15 [22–24]. SiO_2-immobilized Cu-indaBOX catalysts have also been obtained by covalent bonding with alkyl chains to the surface and applied to asymmetric Diels–Alder reactions [25–27]. The activity and selectivity of those immobilized catalysts greatly depends on the structures and environments of active metal species on the surfaces. The chemical and spatial design of catalytically active metal complexes on surfaces is a key issue in the development of heterogeneous asymmetric catalysts.

Recently, we discovered chiral self-dimerization of metal complexes on a SiO_2 surface to realize asymmetric oxidative coupling of 2-naphthol to BINOL [28–31]. We also found that

* Corresponding author. Fax: +81 3 5800 6892.
E-mail address: iwasawa@chem.s.u-tokyo.ac.jp (Y. Iwasawa).

0021-9517/$ – see front matter
doi:10.1016/j.jcat.2006.10.006

the chiral catalysis of Cu-BOX complexes immobilized on SiO_2 for asymmetric Diels–Alder reactions is promoted by surface functionalization with achiral silane-coupling reagents [31,32]. The functionalized surfaces act not only as a simple support for metal complexes, but also as a regulator for chiral reaction space. In this paper, we report the details of preparation, characterization, and enantioselective performances of the surface-functionalized Cu-BOX complex catalysts on a SiO_2 surface. The surface functionalization of SiO_2 with achiral organic molecules without any chiral center dramatically promoted the enantioselectivity of the asymmetric Diels–Alder reaction between cyclopentadiene and 3-acryloyl-2-oxazolidinone on the SiO_2-supported Cu-BOX catalyst.

2. Experimental

2.1. Materials

All chemicals were purchased and used without further purification. 2,2′-Methylenebis[(4*S*)-4-*tert*-butyl-2-oxazoline] (*t*-Bu-BOX) (**1**), copper trifluoromethanesulfonate ($Cu(OTf)_2$), and $Cu(ClO_4)\cdot 6H_2O$ were purchased from Aldrich. Absolute dichloromethane, 1,4-dioxane, tetrahydrofuran, triethylamine, pentane, toluene, *N*,*N*-dimethylformamide, chloroform, and ethanol were purchased from WAKO Chemicals. Isocyanic acid 3-(triethoxysilyl)-propyl ester was purchased from TCI, and all silane-coupling reagents were purchased from Shin-Etsu Silicones.

2.2. Synthesis of a functionalized BOX ligand

The bridge-methylene of *t*-Bu-BOX (**1**) was converted to 2,2-bis[(4*S*)-4-(1,1-dimethylethyl)-4,5-dihydro-2-oxazolyl]-1,3-propanediol (**2**) and then [3-(triethoxysilyl)propyl]-carbamic acid 2,2-bis[(4*S*)-4-(1,1-dimethylethyl)-4,5-dihydro-2-oxazolyl]-1,3-propanediol ester (**3**) similar to the method reported previously [25], as described briefly below.

2.2.1. Synthesis of 2,2-bis[(4S)-4-(1,1-dimethylethyl)-4,5-dihydro-2-oxazolyl]-1,3-propanediol (2)

t-Bu-BOX (**1**) (1.0 g) was dissolved in CH_2Cl_2 (14 ml) together with 0.3272 g of paraformaldehyde. 1,4-Dioxane (3.7 ml) and H_2O (0.68 ml) were added to the solution; then a THF solution (10.7 ml) of triethylamine (1.48 ml) was dropped over 1 h, resulting in a light-yellow solution. After further stirring for 3 days at room temperature, the solution was dropped into cooled pentane, forming white solid precipitates. After filtration and drying under vacuum, white crystalline **2** was obtained (yield 72%). ^{1}H ($CDCl_3$, 270 MHz) [33]: 4.19 (2H, dd, $J = 10.3, 8.9$), 4.06 (2H, dd, $J = 8.9, 8.1$), 4.01 (4H, s), 3.87 (2H, dd, $J = 10.3, 7.6$), 0.86 (18H, s). ^{13}C ($CDCl_3$, 125 MHz) [34]: 165.48, 74.7, 68.7, 63.7, 49.5, 33.5, 25.6. Elemental analysis (found (calculated)): C 61.58% (62.55%), H 9.44% (9.26%), N 8.69% (8.58%).

2.2.2. Synthesis of [3-(triethoxysilyl)propyl]-carbamic acid 2,2-bis[(4S)-4-(1,1-dimethylethyl)-4,5-dihydro-2-oxazolyl]-1,3-propanediyl ester (3)

A 0.3-g sample of **2** was dissolved in absolute DMF (4.2 ml) and triethylamine (0.51 ml). Isocyanic acid (triethoxysilyl)propyl ether (0.5 ml) was added to the solution in a dropwise manner over 5 h. The solution was stirred for 4 days, and a light-yellow solution was obtained. A polystyrene-NH_2 resin was added to the solution, followed by stirring for 1 day. The resin was filtrated, and the filtrate was evaporated and then dried under vacuum. Light-yellow oil was obtained. ^{1}H-NMR (CD_3CN, 500 MHz): 4.46–4.38 (4H, br), 4.13–4.03 (6H, br), 3.75 (6H), 3.01 (2H), 1.46 (2H), 1.16 (9H, s), 0.83 (18H, s), 0.54 (2H). ^{13}C-NMR (CD_3CN, 125 MHz): 163.0, 158.2, 75.2, 68.2, 61.2, 58.0, 48.6, 43.4, 33.5, 25.6, 18.2, 7.4. ^{29}Si-NMR (CD_3CN, 99 MHz): −44.9. Elemental analysis (found (calculated)): C 51.45% (54.12%), H 8.80% (8.84%), N 6.45% (6.82%).

2.3. Immobilization of 3 on SiO_2

SiO_2 (Aerosil 200, Degussa, surface area: 200 $m^2\,g^{-1}$) was calcined at 673 K for 2 h before use as support. A given amount of the functionalized BOX ligand **3** was immobilized on the SiO_2 in absolute toluene under the reflux condition at 388 K for 18 h under N_2 atmosphere. After filtration and washing with absolute CH_2Cl_2, the sample **4** was dried under vacuum at room temperature.

2.4. Achiral functionalization of the BOX-immobilized SiO_2 surface (4)

Each silane-coupling reagent [*p*-styryltrimethoxysilane (**a**), 3-cyclohexylaminopropyltrimethoxysilane (**b**), 3-phenylaminopropyltrimethoxysilane (**c**), ureidopropyltriethoxysilane (**d**), triethoxyvinylsilane (**e**), 3-glycidoxypropyltrimethoxysilane (**f**), 3-(2-aminoethylaminopropyl)trimethoxysilane (**g**), octyltriethoxysilane (**h**), octadecyltriethoxysilane (**i**), or 3-methacryloxypropyltrimethoxysilane (**j**)] was interacted with **4** in absolute toluene under the reflux condition at 388 K for 24 h under N_2 atmosphere. After filtration and washing with CH_2Cl_2, the sample thus obtained was dried under vacuum. The loading of surface-functionalized groups was controlled in the range of 0.3–0.6 mmol g^{-1}.

2.5. Coordination of Cu to the SiO_2-immobilized BOX ligands

An equivalent amount of $Cu(CF_3SO_3)_2$ ($Cu(OTf)_2$) or $Cu(ClO_4)_2\cdot 6H_2O$ to that of the immobilized BOX ligand was interacted with **4** before and after the surface functionalization in absolute CH_2Cl_2 under N_2 atmosphere, and the suspension was stirred for 1 day. After evaporation of the solvent, the obtained sample was dried under vacuum for 1 day.

2.6. Catalyst characterization

2.6.1. FTIR

FTIR spectra for the samples were recorded on a JEOL JIR-100 spectrometer at 298 K. A self-supporting wafer of each sample was placed on a holder at the center of an in situ IR cell with two NaCl windows under N_2 atmosphere.

2.6.2. ^{29}Si solid-state MAS NMR

^{29}Si solid-state MAS NMR spectra were recorded on a Chemagnetics CMX-300 spectrometer operating at 59.67 MHz. The samples were set in a 5-mm-diameter zirconia rotor with kel-F caps and rotated at 4 kHz. Chemical shifts were corrected with the peak of tetramethylsilane.

2.6.3. UV/vis

UV/vis spectra for homogeneous Cu-BOX complexes were measured on a Hitachi U-3500 in a transmission mode. Diffuse-reflectance (DR)-UV/vis spectra for supported Cu-BOX complexes were measured on a JASCO model V-550-DS spectrometer at room temperature. The supported Cu-BOX complexes were enclosed in a thin quartz cell with a stopcock under N_2 atmosphere and evacuated under vacuum without exposure air.

2.6.4. ESR

ESR X-band spectra for $Cu(ClO_4)_2{\cdot}6H_2O$ and supported Cu-BOX catalysts (**5** and **6j**) were recorded on a JEOL JES-RE2X spectrometer at 6 K. MnO_2 was used for the calibration.

2.6.5. XAFS

XAFS spectra at Cu K-edge were measured at the BL-12C station at Photon Factory of the Institute of Material Structure Science, High-Energy Accelerator Research Organization (KEK-IMSS-PF) (proposed no. 2004G081). The homogeneous complex was measured in a transmission mode, and the supported Cu-BOX complexes were measured in a fluorescence mode with a Lytle detector at room temperature. X-rays from the storage ring (2.5 GeV) were monochromatized with a Si(111) double-crystal monochromator. The EXAFS spectra were analyzed with the UWXAFS package [35]. The threshold energy E_0 was set at the inflection point of the absorption edge. Background was subtracted by the AUTOBK program, and the obtained k^3-weighted EXAFS oscillation was Fourier transformed into R-space. Curve-fitting analysis in the R-space was carried out using the FEFFIT program. Phase shifts and backscattering amplitudes were calculated by the FEFF8 code [36].

2.7. Asymmetric Diels–Alder reactions

Cu-BOX catalysts (Cu: 0.35×10^{-3} moll^{-1}) and 3-acryloyl-2-oxazolidinone (3.5×10^{-3} moll^{-1}) were dissolved in dry CH_2Cl_2 (10 ml), and the solution was stirred to obtain a uniform suspension at 298 K. The solution was cooled to the reaction temperature (263 K), after which cyclopentadiene (10.5×10^{-3} moll^{-1}) was added to the solution. The products were analyzed by HPLC (Daicel Chiral OD-H; column temp.: 308 K; n-hexane/2-propanol = 90/10; flow rate: 1.0 ml min^{-1}; detected on a UV/vis spectrometer (254 nm) and a polarimeter for optical rotations of endo-(S)-(−) at 15.50 min and endo-(R)-(+) at 16.94 min [10].

3. Results

3.1. ^{29}Si NMR and FT-IR spectra for the SiO_2-supported BOX ligand (**4**)

The functionalized BOX ligand **3** was immobilized on SiO_2 via the reaction of the $Si(OC_2H_5)_3$ groups of **3** with the surface silanol groups, as shown in Scheme 1. The chemical shifts and assignments of ^{29}Si NMR spectra for the samples **3**, **4**, **j**, and **6j** are listed in Table 1. The chemical shift for the $Si(OC_2H_5)_3$ group of **3** was observed at −44.9 ppm, whereas three peaks at −49.2, −58.6, and −68.2 ppm were observed with the SiO_2-supported BOX ligand **4**. The difference of about 10 ppm in the peak shifts is related to the number of –OR (R: alkyl) and –OSi– [37], which indicates that the BOX ligand **3** was immobilized on the SiO_2 surface with Si–O–Si covalent bonds.

Table 2 shows IR vibrational modes for the BOX ligand **1** impregnated on SiO_2 and the SiO_2-supported functionalized BOX ligand **4**. Fig. 1 shows FTIR spectra for the supported BOX ligand **4**, the surface-functionalized Cu-BOX complex **6j**, methacryloxypropyltrimethoxysilane (**j**) supported on SiO_2, and **j** (neat) in the $\nu_{C=N}$, $\nu_{C=O}$, and δ_{N-H} region. In the spectrum of **1**, $\nu_{C=N}$ was observed at 1657 cm^{-1}, which is similar to $\nu_{C=N}$ for BOX ligand **1** reported previously [38]. For the SiO_2-supported functionalized BOX ligand **4** with amide groups $\nu_{C=O}$ at 1706 cm^{-1} and δ_{N-H} at 1535 cm^{-1} were observed in addition to $\nu_{C=N}$ at 1665 cm^{-1} (Table 2; Fig. 1). We estimated the loading of the functionalized BOX ligand **4** on the surface to be 0.03 mmol g^{-1} by the intensity (peak area) of δ_{C-H} peak at 1370 cm^{-1}.

Table 1
Chemical shifts of ^{29}Si NMR for the functionalized BOX ligand (**3**), the supported BOX ligand (**4**), the 3-methacryloxypropyltrimethoxysilane (**j**), and the surface-functionalized Cu-BOX complex (**6j**)

Sample	Functional group	Chemical shift (ppm)
Functionalized BOX ligand (**3**)[a]	$-Si(OC_2H_5)_3$	−44.9
Supported BOX ligand (**4**)[b,c]	$-Si(OC_2H_5)_2(OSi)$	−49.2
	$-Si(OC_2H_5)(OSi)_2$	−58.6
	$-Si(OSi)_3$	−68.2
3-Methacryloxypropyltrimethoxysilane (**j**)[a]	$-Si(OCH_3)_3$	−58.5
Surface-functionalized Cu-BOX complex (**6j**)[b,d]	$-Si(OCH_3)_2(OSi)$	−68.6
	$-Si(OCH_3)(OSi)_2$	−77.2
	$-Si(OSi)_3$	−82.3

[a] Liquid-phase NMR in CD_3CN.
[b] Measured by solid-state MAS NMR.
[c] Loading of the BOX ligand was 0.15 mmol g^{-1}.
[d] Loading of the silane-coupling reagent **j** was 0.6 mmol g^{-1}.

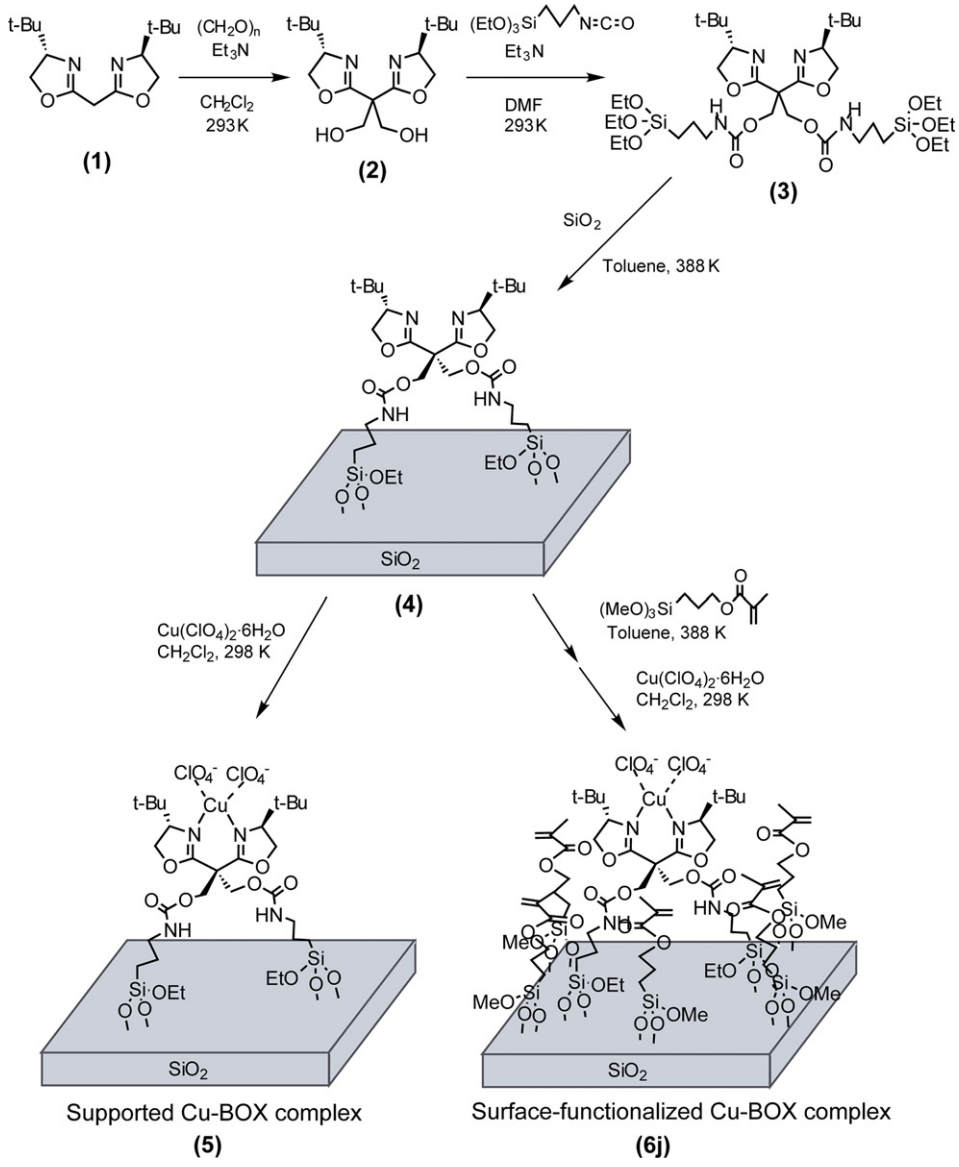

Scheme 1. Preparation steps for the SiO_2-supported Cu-BOX complex (**5**) and the surface-functionalized SiO_2-supported Cu-BOX complex (**6j**).

3.2. UV/vis spectra for the supported Cu-BOX complex (5)

$Cu(OTf)_2$ was mixed with the equivalent amount of BOX ligand in a CH_2Cl_2 solution to form a homogeneous one-to-one BOX-coordinated complex. The one-to-one Cu-BOX complex exhibited a peak at 740 nm, which is larger in wavelength than 640 nm for $Cu(OTf)_2$ [39]. Excess BOX ligand brought about a new significant peak at 595 nm due to the formation of one-to-two Cu-$[BOX]_2$ complex.

In a diffuse-reflectance UV/vis spectrum of the supported Cu-BOX complex **5**, a peak at 370 nm was observed, which is attributed to a $n \rightarrow \pi^*$ transition on a C=N bond of the BOX ligand in **5**. A small peak at around 740 nm was observed for the sample **5**. There was no peak around 595 nm. The complex **5** showed a peak similar to that of a homogeneous $Cu(BOX)(ClO_4)_2$ complex, indicating a structure of **5** similar to that of the homogeneous one-to-one Cu-BOX complex.

3.3. ^{29}Si NMR and FT-IR spectra for the surface-functionalized BOX ligand on SiO_2

Surface functionalization of SiO_2 was performed using 10 silane-coupling reagents (**a**–**j**). 3-Methacryloxypropyltrimethoxysilane (**j**) showed a peak of the $Si(OCH_3)_3$ group at −58.5 ppm in liquid-phase NMR (Table 1). The Cu-BOX complex on SiO_2 functionalized with **j** showed three peaks at −69, −77, and −82 ppm, attributed to three attached Si species of $–Si(OCH_3)_2(OSi)$, $–Si(OCH_3)(OSi)_2$, and $–Si(OSi)_3$, respectively. The NMR data revealed that the silane-coupling reagents were bound covalently on SiO_2.

The $\nu_{C=N}$ (1668 cm^{-1}) peak of the surface-functionalized Cu-BOX complex **6j** was almost the same as those of the supported BOX ligand **4** (1665 cm^{-1}), indicating that no structural change at the BOX unit occurred via the surface functionalization with **j** (Table 2). 3-Methacryloxypropyltrimethoxysilane (**j**) showed three vibrations of $\nu_{C=O}$ (1720 cm^{-1}), $\nu_{C=C}$

Table 2
IR wavenumbers for the BOX ligand (**1**) impregnated on SiO_2, the supported BOX ligand (**4**), the silane-coupling reagent (**j**), SiO_2-immobilized silane-coupling reagent (**j**), and the surface-functionalized Cu-BOX complex (**6j**)

Vibration mode	BOX ligand (**1**) [38] (cm^{-1})	BOX ligand (**1**) on SiO_2[a] (cm^{-1})	SiO_2-supported BOX ligand (**4**) (cm^{-1})
$\nu_{(C=N)}$ (BOX)	1670	1657	1665
$\nu_{(C=O)}$ (O–CO–NH)	–	–	1706
$\delta_{(N-H)}$ (O–CO–NH)	–	–	1535
$\delta_{(C-H)}$ (BOX)	1470, 1400, 1365	1480, 1402, 1371	1481, 1370
$\delta_{(C-H)}$ (–$(CH_2)_3$–)	–	–	1448, 1398
Vibration mode	**Methacryloxypropyl-trimethoxysilane (j) (neat) (cm^{-1})**	**SiO_2-supported methacryloxypropyl-trimethoxysilane (j)[b] (cm^{-1})**	**Surface-functionalized SiO_2-supported Cu-BOX complex (6j) (cm^{-1})**
$\nu_{(C=O)}$ (O–CO–C(=C)(CH_3))	1720	1701, 1720	1704, 1722[c]
$\nu_{(C=C)}$ (O–CO–C(=C)(CH_3))	1638	1639	1635
$\delta_{(C-H)}$ (O–CO–C(=C)(CH_3))	1453, 1441	1456, 1442	1456, 1444
$\nu_{(C=N)}$ (BOX)	–	–	1668
$\delta_{(N-H)}$ (O–CO–NH)	–	–	1529

[a] The BOX ligand **1** was impregnated with SiO_2 (Aerosil 200).
[b] The silane-coupling reagent **j** was immobilized on SiO_2 (Aerosil 200).
[c] Shouldered.

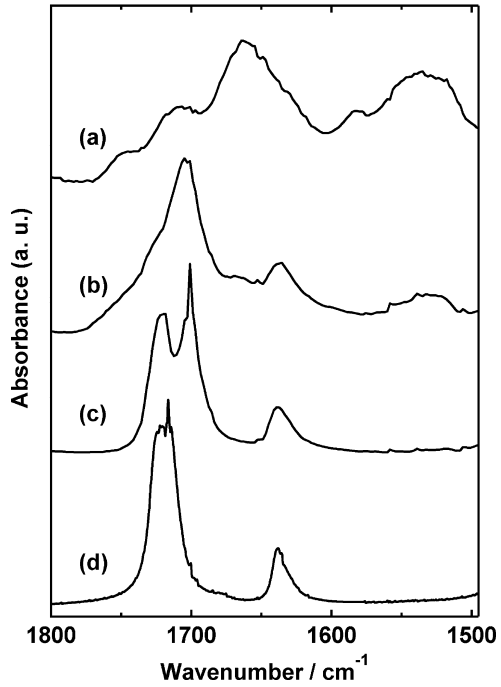

Fig. 1. IR spectra at 298 K for (a) the supported BOX ligand (**4**), (b) the surface-functionalized Cu-BOX complex (**6j**), (c) methacryloxypropyltrimethoxysilane (**j**) supported on SiO_2, and (d) methacryloxypropyltrimethoxysilane (**j**) (neat). The loading of BOX ligand was 0.06 mmol g^{-1} on (a), and 0.03 mmol g^{-1} on (b), respectively. The loadings of **j** on (b) and (c) were 0.6 mmol g^{-1}.

(1638 cm^{-1}), and δ_{C-H} (1453, 1441 cm^{-1}), as shown in Table 2. The surface-functionalized Cu-BOX complex **6j** also showed $\nu_{C=O}$ at 1704 cm^{-1}, $\nu_{C=C}$ at 1635 cm^{-1}, and δ_{C-H} at 1456 and 1444 cm^{-1} due to the vibrational modes of the immobilized **j**. The δ_{N-H} peak (1535 cm^{-1}) of **4** shifted to 1529 cm^{-1} for **6j**, although there was a large error bar in these peak positions due to their broad peaks.

The amount of immobilized **j** on the surface was estimated using the δ_{C-H} peak area. The estimated coverage of immobilized species **j** on SiO_2 increased to 0.6 mmol g^{-1} by increasing the amount of **j** used for the preparation, and the coverage of **j** did not increase any further by further increases in **j**. Thus the maximum coverage of the immobilized **j** on the SiO_2 surface was suggested to be 0.6 mmol g^{-1}, corresponding to 2 molecules nm^{-2}.

3.4. Loading and valence of Cu complexes on the surface by XRF and XPS

The loadings of Cu for the supported Cu-BOX complexes **5** and **6j** were examined by XRF. When 0.03 mmol g^{-1} of the immobilized BOX ligand **4** was used, the Cu loading in the supported Cu-BOX complex **5** was 0.19 wt%, which is equivalent to the amount of the immobilized BOX ligand on SiO_2. The Cu quantity in the surface-functionalized Cu-BOX complex **6j** was also similar (0.16 wt%). Thus the Cu precursor $Cu(ClO_4)_2{\cdot}6H_2O$ reacted with the immobilized BOX ligand to form one-to-one complexes, and the supported Cu-BOX complexes were dispersed on the surface with the surface density of 0.1 nm^{-2}.

XPS binding energies for Cu(BOX)$(OTf)_2$ and the SiO_2-supported Cu(BOX)$(OTf)_2$ complex are given in Table 3. Cu $2p_{3/2}$ peaks for the two complexes were observed at 933.5 and 933.6 eV, respectively, which are attributed to Cu^{2+} species [40]. The supported Cu(BOX)$(ClO_4)_2$ complex **5** and the surface-functionalized Cu(BOX)$(ClO_4)_2$ complex **6j** showed similar binding energies, 933.6 and 933.7 eV, respectively, which are also assigned as bivalent Cu species (Table 3).

3.5. ESR spectra for 5 and 6j

ESR spectra for $Cu(ClO_4)_2{\cdot}6H_2O$ and the supported Cu-BOX complexes **5** and **6j** were measured at 6 K, as shown in Fig. 2 and Table 4. The g values were $g_{\parallel} = 2.286$ ($A_{\parallel} =$ 13.4 mT) and $g_{\perp} = 2.071$ for **5** and $g_{\parallel} = 2.284$ ($A_{\parallel} = 13.6$ mT)

Table 3
Binding energies of Cu 2p and N 2p for homogeneous and supported $Cu(BOX)(OTf)_2$ complexes, the supported $Cu(BOX)(ClO_4)_2$ complex (**5**), surface-functionalized $Cu(BOX)(ClO_4)_2$ complex (**6j**), and Cu references measured by XPS

Sample	Cu $2p_{1/2}$	Cu $2p_{3/2}$	N 2p
$Cu(BOX)(OTf)_2$ complex[a]	953.8	933.5	400.0
Supported $Cu(BOX)(OTf)_2$ complex[a]	953.8	933.6	399.9
Supported $Cu(BOX)(ClO_4)_2$ complex (**5**)[b]	–	933.6	–
Surface-functionalized $Cu(BOX)(ClO_4)_2$ complex (**6j**)[b]	–	933.7	–
Cu (metal) [40]	–	932.7	–
Cu_2O[a]	–	932.4	–
CuO[a]	–	933.8	–

[a] The binding energies were referred to 284.8 eV of C 1s peak.
[b] The binding energies were referred to 103.5 eV of Si 2p and 533.0 eV of O 1s peaks.

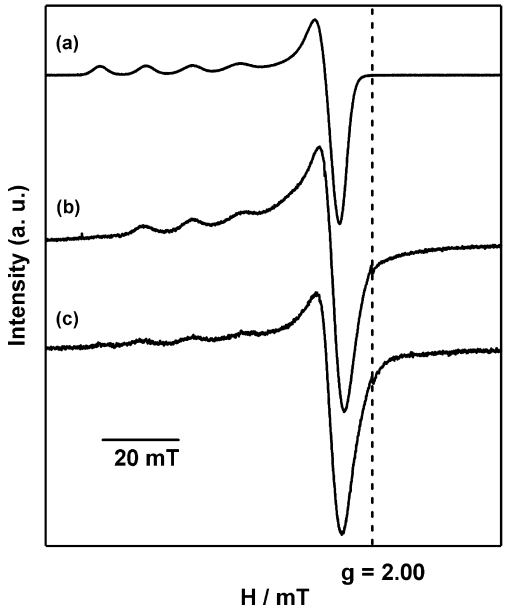

Fig. 2. ESR spectra measured at 6 K for (a) $Cu(ClO_4)_2{\cdot}6H_2O$ in acetone, (b) the supported $Cu(BOX)(ClO_4)_2$ complex (**5**) in CH_2Cl_2, and (c) the surface-functionalized $Cu(BOX)(ClO_4)_2$ complex (**6j**) in CH_2Cl_2.

Table 4
ESR structural parameters for $Cu(ClO_4)_2{\cdot}6H_2O$, the supported $Cu(BOX)(ClO_4)_2$ complex (**5**) and the surface-functionalized $Cu(BOX)(ClO_4)_2$ complex (**6j**) recorded at 6 K

Sample	$g_{\parallel}$	$A_{\parallel}$ (mT)	$g_{\perp}$	g_{av}
$Cu(ClO_4)_2{\cdot}6H_2O$[a]	2.400	12.6	2.081	2.187
5[b]	2.286	13.4	2.071	2.143
6j[b]	2.284	13.6	2.070	2.141

[a] Measured in acetone.
[b] Measured in CH_2Cl_2.

and $g_{\perp} = 2.070$ for **6j**. The g_{av} values were 2.143 for **5** and 2.141 for **6j**. The spectrum shown in Fig. 2b indicates that the Cu ion in the supported Cu-BOX complex **5** is situated in a four-coordinated square-planar symmetry [41]. The ESR signal for **5** was observed in a higher magnetic field than that for $Cu(ClO_4)_2{\cdot}6H_2O$, as shown in Fig. 2. It is known that when Cu^{2+} ions are coordinated with bidentate nitrogen ligands, their Cu^{2+} ESR signals are observed at higher magnetic fields than those before coordination [42]. These results demonstrate that the Cu precursor was coordinated with the immobilized BOX ligand on the surface. Fig. 2c for **6j** shows a similar spectrum to that for **5**, indicating that the Cu complex of **6j** has a similar configuration to that of **5**.

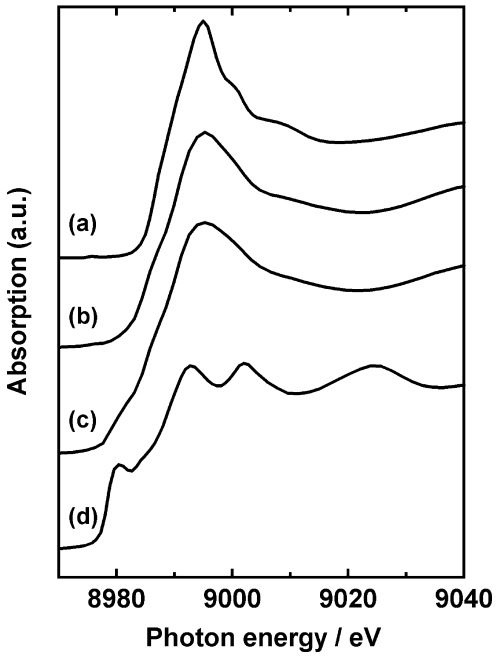

Fig. 3. Cu K-edge XANES spectra for (a) the $Cu(ClO_4)_2{\cdot}6H_2O$ precursor, (b) the supported $Cu(BOX)(ClO_4)_2$ complex (**5**), (c) the surface-functionalized $Cu(BOX)(ClO_4)_2$ complex (**6j**), and (d) Cu foil.

3.6. XANES spectra for *5* and *6j*

Fig. 3 shows Cu K-edge XANES spectra for both **5** and **6j**, demonstrating a very weak peak at 8977.5 eV. This peak is attributed to the dipole-forbidden 1s → 3d transition of bivalent Cu^{2+} [43]. Both **5** and **6j** exhibited shoulder peaks at 8985.1 eV, which are assigned to the Cu 1s → $4p_z$ transition accompanied by a simultaneous ligand-to-Cu^{2+} charge-transfer (CT) excitation particular to Cu^{2+} species elongated to the z-axis [44]. A similar shoulder was also observed for $Cu(ClO_4)_2{\cdot}6H_2O$, but its peak position of 8987.3 eV was higher than those for **5** and **6j**, indicating that the Cu^{2+} ions in **5** and **6j** interact with the BOX ligands covalently.

3.7. EXAFS spectra for *5* and *6j*

The structural parameters for $Cu(BOX)(ClO_4)_2$ and supported Cu-BOX complexes **5** and **6j** were determined by Cu K-edge EXAFS analysis. Fig. 4 shows the EXAFS oscillations and their associated Fourier transforms. The curve-fitting results are summarized in Table 5. Because the number of

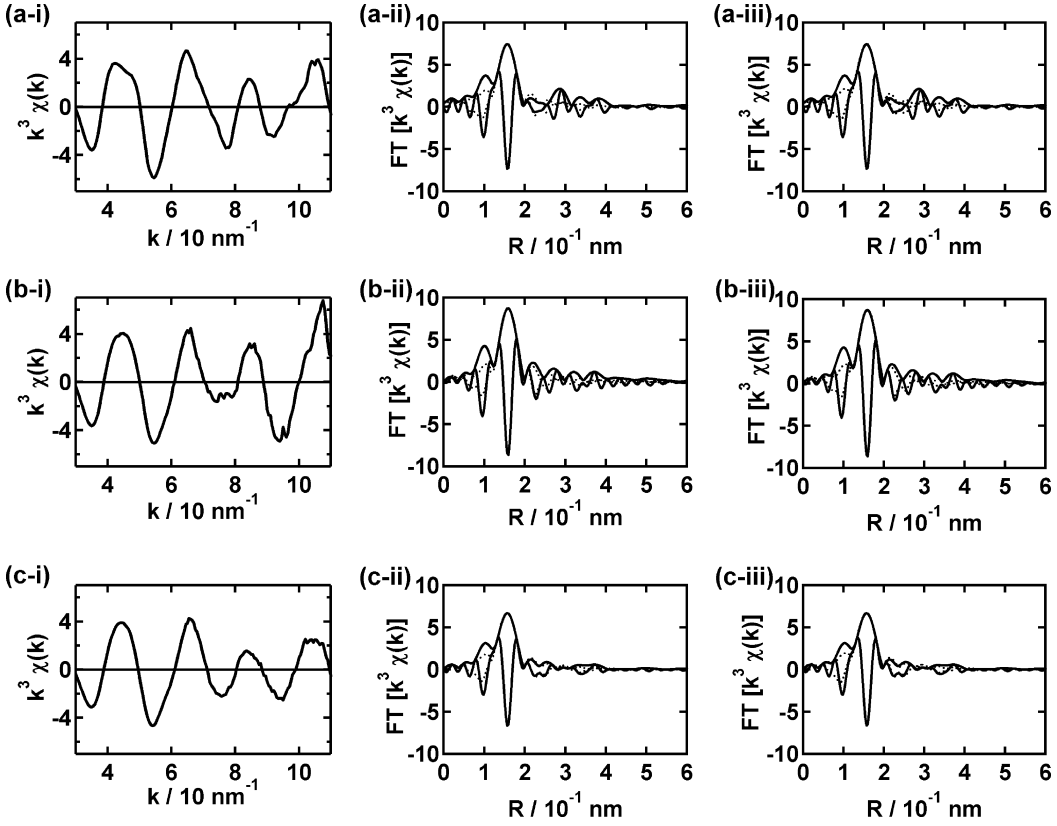

Fig. 4. Cu K-edge k^3-weighted EXAFS oscillations (i), their associated Fourier transforms and curve-fittings with a Cu–O shell (ii), and curve-fittings with a Cu–N shell (iii) at 298 K for (a) $Cu(BOX)(ClO_4)_2$, (b) supported Cu-BOX complex (**5**), and (c) surface-functionalized Cu-BOX complex (**6j**). Solid lines and dotted lines in the Fourier transforms represent observed data and fitted curves of absolute and imaginary parts, respectively.

Table 5
Structural parameters determined by curve-fitting of the EXAFS Fourier transforms at Cu K-edge measured at 293 K for the $Cu(BOX)(ClO_4)_2$ precursor, the supported $Cu(BOX)(ClO_4)_2$ complex (**5**), and the surface-functionalized $Cu(BOX)(ClO_4)_2$ complex (**6j**)[a]

Shell	CN	R (nm)	σ^2 (nm^2)		
			Homogeneous precursor		
Cu–O[b]	3.7 ± 0.6	0.196 ± 0.001	$(4 \pm 2) \times 10^{-5}$	$\Delta E_0 = 10 \pm 2$ eV,	$R_f = 1.62\%$
Cu–N[c]	4.5 ± 0.6	0.198 ± 0.001	$(4 \pm 1) \times 10^{-5}$	$\Delta E_0 = 9 \pm 2$ eV,	$R_f = 1.26\%$
			Supported catalyst (**5**)		
Cu–O[b]	3.6 ± 0.5	0.197 ± 0.002	$(2 \pm 1) \times 10^{-5}$	$\Delta E_0 = 12 \pm 2$ eV,	$R_f = 1.10\%$
Cu–N[c]	4.4 ± 0.5	0.199 ± 0.001	$(2 \pm 1) \times 10^{-5}$	$\Delta E_0 = 11 \pm 1$ eV,	$R_f = 0.74\%$
			Surface-functionalized catalyst (**6j**)		
Cu–O[b]	3.4 ± 0.5	0.195 ± 0.001	$(4 \pm 1) \times 10^{-5}$	$\Delta E_0 = 10 \pm 2$ eV,	$R_f = 1.23\%$
Cu–N[c]	4.1 ± 0.5	0.198 ± 0.001	$(4 \pm 1) \times 10^{-5}$	$\Delta E_0 = 9 \pm 2$ eV,	$R_f = 0.92\%$

[a] $k = 30$–100 nm^{-1}, $R = 0.11$–0.20 nm.
[b] Fitted with a Cu–O shell.
[c] Fitted with a Cu–N shell.

permitted independent parameters for the curve-fitting is estimated as 6 [45], we performed EXAFS curve-fitting analysis for one shell, Cu–O or Cu–N (Table 5). When the contribution to the EXAFS scattering was assumed to be the Cu–O bond, then the coordination number (CN) and bond distance (R) for $Cu(BOX)(ClO_4)_2$ were 3.7 ± 0.6 and 0.196 ± 0.001, respectively, and when the contribution was assumed to be the Cu–N bond, then these values were 4.5 ± 0.6 and 0.198 ± 0.001, respectively. The actual CN for $Cu(BOX)(ClO_4)_2$ was 4 (two Cu–O bonds and two Cu–N bonds), which is an CN intermediate value obtained by curve fitting.

In the supported Cu-BOX complexes **5** and **6j**, a similar local coordination to that for $Cu(BOX)(ClO_4)_2$ was observed, as shown in Table 5. The CN and R for **5** were 3.6 ± 0.5 and 0.197 ± 0.002 nm, respectively, in the fitting with Cu–O and 4.4 ± 0.5 and 0.199 ± 0.001 nm, respectively, in the fitting with Cu–N. The results indicate that the supported Cu-BOX complexes have a similar structure to that of $Cu(BOX)(ClO_4)_2$. Similar CN and R values were also observed for the surface-functionalized catalyst **6j**. Thus the local structures around Cu in the supported Cu-BOX catalysts are similar to those in $Cu(BOX)(ClO_4)_2$, as shown in Scheme 1.

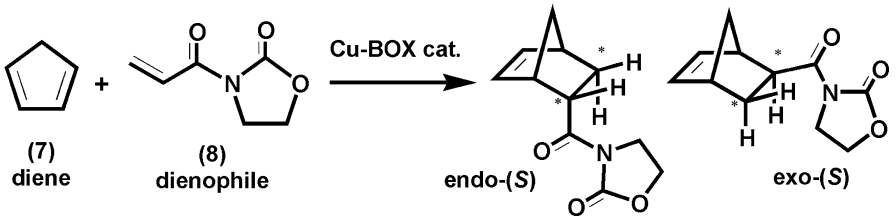

Scheme 2. Asymmetric Diels–Alder reaction between cyclopentadiene (**7**) and 2-acryloyl-2-oxazolidinone (**8**).

Table 6
Catalytic performances of the homogeneous and supported Cu-BOX catalysts for asymmetric Diels–Alder reaction

Catalyst	Solvent	Temperature (K)	Time (h)	Conv. (%)	Endo%	Ee(*S*)% of endo
Homogeneous catalysts						
$Cu(BOX)(OTf)_2$[a]	CH_2Cl_2	263	4	98	88	27
$Cu(BOX)(ClO_4)_2$[a]	CH_2Cl_2	263	3	98	89	5
$Cu(BOX)(ClO_4)_2$	CH_2Cl_2	263	1	4	89	5
$Cu(BOX)(ClO_4)_2$[b]	CH_2Cl_2	263	1	3	94	6
Supported catalysts						
$Cu(BOX)(OTf)_2$[c]	CH_2Cl_2	263	6	60	95	7
5	CH_2Cl_2	263	1	61	90	15
			24	100		14
5[d]	CH_2Cl_2	263	1	58	90	15
			24	100		13
6j[e]	CH_2Cl_2	263	1	12	91	49
			24	100		42
6j[f]	CH_2Cl_2	263	1	16	93	65
			24	100		63
6j[f,g]	CH_2Cl_2	263	24	88	93	58
6j[f]	Toluene	263	24	100	91	38
6j[f]	$CHCl_3$	263	24	88	92	0.8
6j[f]	Ethanol	263	24	86	90	5

Cu/diene/dienophile = 1/30/10, concentration of Cu was 0.35 mmol l^{-1}.
[a] Concentration of Cu was 25 mmol l^{-1}.
[b] 2,2′-Isopropylidene-bis[(4*S*)-4-*tert*-butyl-2-oxazoline] (**9**) was used.
[c] Concentration of Cu was 0.40 mmol l^{-1}.
[d] 3-Methacryloxypropyltrimethoxysilane (**j**) was added into the reaction solution.
[e] Loading of **j** was 0.3 mmol g^{-1}.
[f] Loading of **j** was 0.6 mmol g^{-1}.
[g] Reused.

3.8. Asymmetric Diels–Alder reactions catalyzed by Cu-BOX complexes

Asymmetric Diels–Alder reactions between cyclopentadiene (**7**) and 3-acryloyl-2-oxazolidinone (**8**) (Scheme 2) were conducted on homogeneous and supported Cu-BOX complexes (Table 6). The homogeneous $Cu(BOX)(ClO_4)_2$ showed low enantioselectivity (5% ee), and deactivation of the catalytic activity was observed. $Cu(BOX)(OTf)_2$ in a homogeneous phase showed higher enantioselectivity (27% ee) than that on $Cu(BOX)(ClO_4)_2$ under the similar reaction conditions.

The immobilization of Cu-(BOX) complex on SiO_2 brought about an increase in the catalytic activity from 4 to 61% conversion at 1 h reaction, and the catalytic reaction on the supported Cu-BOX complex catalyst (**5**) was completed after 24 h, as shown in Table 6. However, the enantioselectivity of the supported Cu-BOX complex catalysts was still as low as 15% ee for $Cu(BOX)(ClO_4)_2$ and 7% ee for $Cu(BOX)(OTf)_2$. Endoselectivity was 95% for the latter complex (Table 6). When the BOX ligand **1** was replaced by the ligand **9**, the conversion and enantioselectivity in the homogeneous phase were also low (3% conversion, 6% ee).

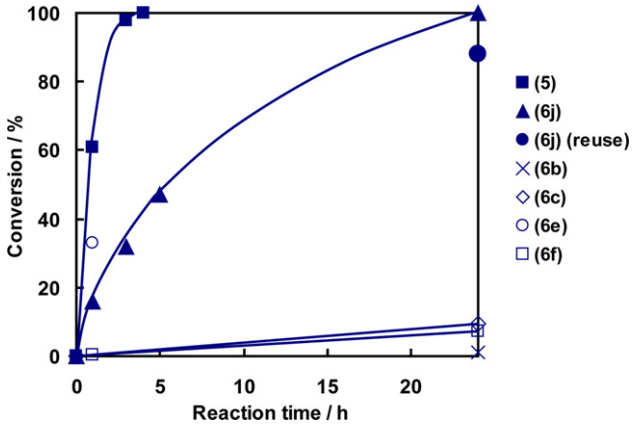

Fig. 5. The catalytic activities (conversion) of **5**, **6b**, **6c**, **6e**, **6f**, **6j**, and **6j** (reuse) as representative samples at 263 K in CH_2Cl_2. Cu/diene/dienophile = 1/30/10, concentration of Cu was 0.35 mmol l^{-1}. Loading of **j** on **6j** was 0.6 mmol g^{-1}.

The catalytic activity (conversion) decreased due to the surface functionalization, as shown in Fig. 5, which shows the effects of typical immobilized silane-coupling reagents on the conversion. It was found that the surface functionalization with achiral silane-coupling reagents increased the enantioselectivity. Fig. 6 shows the catalytic performance of the surface-functionalized Cu-BOX catalysts with various silane-coupling reagents. Both the catalytic activity and selectivity of the surface-functionalized catalysts strongly depended on the functionalizing reagents (Fig. 6). 3-Methacryloxypropyltrimethoxysilane (**j**) was the best reagent for increasing the enantioselectivity. The enantioselectivity in the endo product on **6j** with 0.3 mmol g^{-1} of **j** was 49% ee and that on **6j** with 0.6 mmol g^{-1} of **j** was 65% ee, as shown in Table 6. After 24 h, the conversion reached 100%, whereas the enantioselectivity remained at 63% ee on the latter catalyst. The endoselectivity was 91%, similar to those of homogeneous $Cu(BOX)(ClO_4)_2$ complex and supported complex **5**. Furthermore, the surface-functionalized catalyst **6j** could be reused without significant loss of catalytic activity or enantioselectivity (88% conversion and 58% ee of the endo product after 24 h), as shown in Table 6 and Fig. 5. Note that when the silane-coupling reagent with the methacrylate (**j**) was added to the reaction solution on **5**, there was no increase in the enantioselectivity (15% ee of the endo product),

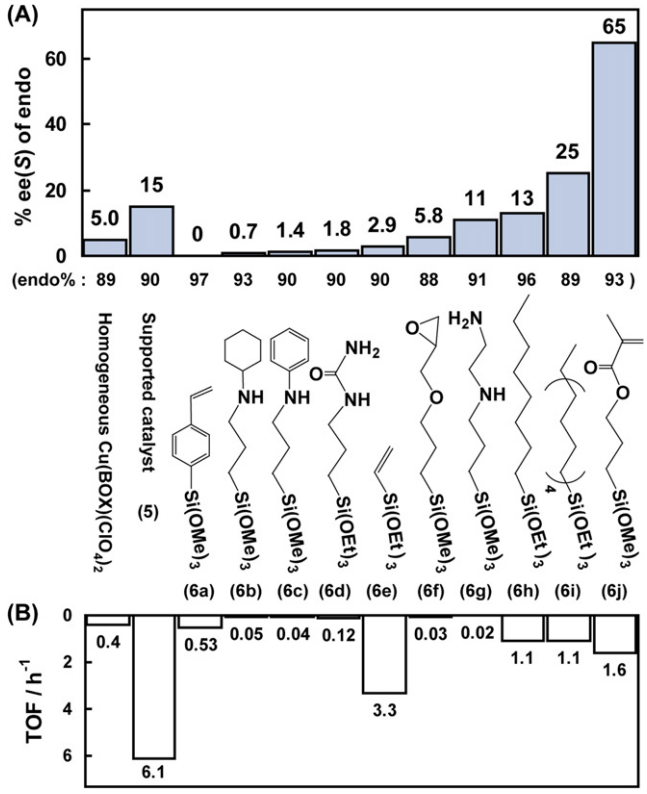

Fig. 6. Catalytic performances of homogeneous $Cu(BOX)(ClO_4)_2$, the supported $Cu(BOX)(ClO_4)_2$ complex (**5**), and the surface-functionalized $Cu(BOX)(ClO_4)_2$ complexes (**6a**)–(**6j**) for asymmetric Diels–Alder reactions of cyclopentadiene (**7**) and 3-acryloyl-2-oxazolidinone (**8**). (A) shows % ee(*S*) of endo. Endo% is represented in the parenthesis. (B) shows TOF (turnover frequency) of the catalytic reaction. TOF is defined as obtained product $Cu^{-1}\ h^{-1}$. Cu: 3.5×10^{-6} mol, cyclopentadiene: 10.5×10^{-5} mol, 3-acryloyl-2-oxazolidinone: 3.5×10^{-5} mol, CH_2Cl_2: 10 ml, 263 K, N_2 atmosphere. The catalytic reactions were monitored by GC-MS and HPLC.

as shown in Table 6, indicating that enantioselectivity promotion is a surface event.

The other silane-coupling reagents with the full coverage loading (0.6 mmol g^{-1}) did not significantly promote enantioselective catalysis. Fig. 6 shows the catalytic performance of the surface-functionalized Cu-BOX complex catalysts used in this study. Styrene (**a**) and vinyl (**e**) groups, which are conjugated hydrocarbon moieties, caused large decreases in enantioselectivity (0% ee and 2.9% ee, respectively). Long alkyl groups, such as the octyl (**h**) and octadecyl (**i**) groups, increased enantioselectivity slightly (13% ee and 25% ee, respectively). The longer octadecyl group (**6i**) showed a higher enantioselectivity (25% ee) than that of the shorter octyl group (**6h**) (13% ee). The other cyclohexylamino (**b**), phenylamino (**c**) (with the product obtained as a mixture), urea (**d**), epoxy (**f**), and amino (**g**) groups significantly decreased the catalytic activities and enantioselectivities to 0.7–11% ee. Among the catalysts functionalized with 10 silane-coupling reagents, only the methacryl-functionalized catalyst (**6j**) showed high enantioselectivity (65% ee of the endo product).

The effects of solvent on the performance of the methacryl-functionalized catalyst (**6j**) were also examined (Table 6). In nonpolar toluene, the enantioselectivity also increased to 38% ee by surface functionalization, whereas polar solvents, such as chloroform and ethanol, did not amplify the enantioselectivity by surface functionalization.

4. Discussion

4.1. Surface structures of SiO_2-supported Cu-BOX complexes

The loading and dispersion of the supported BOX ligands on SiO_2 are key issues in the design of functionalized catalyst surfaces using silane-coupling reagents. From this standpoint, we controlled the surface density of the Cu BOX ligand to be 0.03 mmol g^{-1}, which is equal to 0.1 BOX on 1 nm^2 of SiO_2 surface. The cross-sectional area of a BOX ligand **3** on SiO_2 is estimated to be 1.9 nm^2. These conditions allow us to consider the possibility that the BOX ligands were isolatedly immobilized on SiO_2.

The surface silanol groups on SiO_2 calcined at 673 K were estimated to be about 3 Si–OH nm^{-2} [46], which is a sufficient amount for the further immobilization of silane-coupling reagents after the attachment of the BOX ligands. As mentioned earlier, the maximum loading of **j** was found to be 0.6 mmol g^{-1}, which is equal to 2.0 methacrylate nm^{-2}, where the SiO_2 surface around the BOX ligand is considered fully covered with **j**.

The SiO_2-supported $Cu(BOX)(ClO_4)_2$ complex **5** was more active than the homogeneous $Cu(BOX(1))(ClO_4)_2$ complex for the asymmetric Diels–Alder reaction, as shown in Table 6. However, the local structures of the both complexes had a similar 4-coordinated square-planar geometry, as indicated by ESR and XAFS. In general, simple attachment of metal complexes on oxide surfaces suppresses their catalytic activities, but the present result is in contrast to the general trend. The homogeneous $Cu(BOX)(ClO_4)_2$ complex was deactivated during the catalysis in solution due to its instability under the present conditions. The attachment of the Cu precursor on the immobilized BOX ligand on SiO_2 seems to prevent the decomposition and aggregation of Cu species.

The surface-functionalized Cu-BOX complex **6j** was also characterized by XPS, ESR, and XAFS as described above, which revealed the 4-coordinated structure with bidentate nitrogens of the BOX ligand and two perchloric anions. The coordination sphere around Cu^{2+} ion in **6j** was similar to that in **5** with no significant change by the surface functionalization, as shown in Scheme 1. The methacryl moieties on the surface did not influence the local coordination of $Cu(BOX)(ClO_4)_2$ in the attached Cu complex even when the loading of methacrylate on SiO_2 increased from 0.3 to 0.6 mmol g^{-1}. This was also confirmed by FTIR (Fig. 1), showing that the $\nu_{C=N}$ of BOX did not change due to surface functionalization.

Two ClO_4^- anions were substituted to a dienophile with the two oxygens of carbonyl groups in the catalytic reaction conditions. The most stable angle between the plane of N–Cu–N and that of O–Cu–O in an intermediate BOX-Cu-dienophile complex was calculated to be 39° [47]. These results suggest that the steric interaction between *tert*-Bu groups on BOX and the coordinated dienophile **8** led to a distorted square-planar con-

figuration and promoted the attack of diene **7** to **8** from its α-Re face, resulting in *S*-selectivity of the product.

4.2. Amplification of enantioselectivity by surface functionalization with achiral methacryl reagents

The methacryl-functionalized complex **6j** exhibited the amplification of enantioselectivity for the asymmetric Diels–Alder reaction, as shown in Table 6. The enantioselectivity increased depending on the loading of methacrylate on SiO_2. At the loading of 0.6 mmol g^{-1}at a full coverage of **j** on the surface, the enantioselectivity was amplified from 15 to 65% ee. Note that no increase in enantioselectivity was observed when the methacryl silane-coupling reagent was added to the CH_2Cl_2 solution in which the supported Cu-BOX complex **5** was suspended. No Diels–Alder reactions occurred with the methacryl side chains. There was no significant interaction between the supported Cu-BOX complex on SiO_2 and the methacrylate in solution, so that the enantioselective coordination sphere around Cu^{2+} in **5** cannot be positively changed. Thus the chemical attachment of the silane-coupling reagent on the SiO_2 surface (surface functionalization) is indispensable to promotion of the enantioselective catalysis. It was found that the full-coverage functionalization of SiO_2 surfaces with **j** was most effective for creating the enantioselective reaction field on catalyst **6j**.

4.3. Effects of surface-functionalization with different silane-coupling reagents

The capping of free surface Si–OH groups with trimethylsilyl moieties has been reported to be favorable for asymmetric catalysis on SiO_2, because the silanol groups behave as undesirable reaction sites [25,48]. However, the present results for the styryl- (**6a**) and vinyl- (**6e**) functionalized catalysts indicate that the simple capping of silanol groups did not lead to an increase in enantioselectivity. In the urea- (**6d**), epoxy- (**6f**), and amino- (**6g**) functionalized catalysts, catalytic activity significantly decreased, mainly because these reagents could act as bidentate ligands for Cu^{2+}, which likely decomposed the original Cu-BOX complexes on the SiO_2 surface. Functionalization with cyclohexylamino- (**b**) and phenylamino- (**c**) groups, which have carbon ring structures that prevent the substrates from approaching to Cu^{2+} active center and amino groups that can coordinate to Cu^{2+}, also drastically diminished the activity.

Only the methacryl-functionalized catalyst (**6j**) among the functionalizing reagents used in this study exhibited significant amplification of the enantioselectivity, which indicates a positive effect of the methacryl group on the surface-induced amplification of enantioselectivity. Some weak interaction is suggested by the shift of δ_{N-H} from 1535 to 1529 cm^{-1} by surface functionalization with **j**. The $\nu_{C=O}$ peak at 1720 cm^{-1} for **j** shifted to 1701 cm^{-1} by immobilization on the SiO_2 surface, indicating chemical interaction of **j** with the surface. The peak at 1704 cm^{-1} became major with the immobilized **j** (Fig. 1), indicating that the C=O groups of **j** interact with the SiO_2 surface more preferentially than the immobilized BOX (**4**). Although the precise arrangement of the immobilized **j** on the SiO_2 surface is not clear, the methacryl moiety can positively interact with the NH group of the immobilized BOX (**4**) at the full monolayer of **j**. Thus the immobilized **j** occupies the space around the Cu-BOX complex to enhance *tert*-Bu chirality.

Enhanced enantioselectivity of hydrogenation on homogeneous chiral Rh complexes by the addition of achiral ligands also has been reported [49]. In this case, the achiral ligand coordinated to the Rh center of the complex with the chiral ligands, forming a new chiral complex with the additional ligand under the reaction conditions. Note that the local structure of the Cu-BOX complex on **6j** did not change from **5** due to methacryl functionalization on the surface. The chiral part of the Cu-BOX complex determining the configuration of the product is the bulky *tert*-Bu group on the BOX. The surface-functionalized reagent may behave as glue for the BOX to amplify the enantioselectivity of the Cu-BOX complex on the surface. Because the lengths of the reagent **j** and the BOX ligand on the SiO_2 surface are similar, the methacryl oxygen may easily interact with the NH group of the chiral BOX ligand by hydrogen bonding.

In the asymmetric Diels–Alder reaction (Scheme 2), 3-acryloyl-2-oxazolidinone is coordinated to the Cu-BOX complex with C_2-symmetry, and then cyclopentadiene approaches the dienophile-coordinated Cu-BOX complex. On the SiO_2-supported Cu-BOX catalysts, the approach of cyclopentadiene to the Cu^{2+} ions is regulated by blocking a side of the chiral BOX ligand with the large functionalized SiO_2 surface. The dependency of the enantioselectivity on the coverage of 3-methacryloxypropyltrimethoxysilane (**j**) indicates that the achiral methacryl groups surround the supported chiral BOX ligand to form a novel assembled structure around the chiral BOX ligand. The achiral methacryl groups near the chiral BOX ligand selectively occupy the space below the Cu-BOX complex and increase the bulkiness of *tert*-Bu groups on the BOX ligand by a glue effect, and then the approach of cyclopentadiene to the Cu site is controlled spatially in a chiral direction, resulting in the remarkable increase in the enantioselectivity.

The solvent effect for the enantioselectivity on **6j** supports this suggestion. A large increase in enantioselectivity was observed in nonpolar solvents, such as CH_2Cl_2 and toluene, as shown in Table 6. On the other hand, polar solvents like chloroform and ethanol prevented amplification of the enantioselectivity by surface functionalization. These results suggest that hydrogen bonding between the chiral BOX ligand and the achiral reagent contributes to formation of the novel chiral assembled structure on the surface.

5. Conclusion

We have found significant amplification of enantioselectivity for the asymmetric Diels–Alder reaction on the SiO_2-supported Cu-BOX catalyst prepared by surface functionalization with achiral silane-coupling reagents. The SiO_2-supported Cu-BOX complex was more active than the homogeneous counterpart for the Diels–Alder reaction of cyclopentadiene and 3-acryloyl-2-oxazolidinone. The surface functionalization with achiral

3-methacryloxypropyltrimethoxysilane significantly increased the enantioselectivity for the endo product, from 15 to 65% ee. These findings suggest that the hydrogen bond between the chiral BOX ligand and the achiral methacrylate on the SiO_2 surface led to the creation of a new chiral assembly as a glue effect, which cannot be prepared in solutions. These results provide a new strategy for developing advanced designs in preparing enantioselective heterogeneous catalysts.

Acknowledgments

The authors thank Dr. T. Sasaki at the University of Tokyo for NMR measurements. This work was supported by the 21st century COE program of MEXT. The XAFS measurements were performed in KEK-IMSS-PF with the approval of the Photon Factory Advisory Committee (proposal 2004G081).

References

[1] L. Pu, Chem. Rev. 98 (1998) 2405.
[2] Y. Chen, S. Yetka, A.K. Yudin, Chem. Rev. 103 (2003) 3155.
[3] R. Noyori, Asymmetric Catalysts in the Organic Synthesis, Wiley, New York, 1994.
[4] E.N. Jacobsen, A. Pfaltz, H. Yamamoto (Eds.), Comprehensive Asymmetric Catalysis, Springer, Berlin, 1999.
[5] P. McMorn, G.J. Hutchings, Chem. Soc. Rev. 33 (2004) 108.
[6] K.C. Nicolaou, G. Vassilikogiannakis, W. Magerlein, Angew. Chem. Int. Ed. 41 (2002) 1668.
[7] K. Takao, R. Munakata, K. Tadano, Chem. Rev. 105 (2005) 4779.
[8] D.A. Evans, W.C. Black, J. Am. Chem. Soc. 115 (1993) 4497.
[9] Y. Morimoto, M. Iwahashi, K. Nishida, Y. Hayashi, H. Shirahama, Angew. Chem. Int. Ed. Engl. 35 (1996) 904.
[10] D.A. Evans, S.J. Miller, T. Lectka, P. von Matt, J. Am. Chem. Soc. 121 (1999) 7559.
[11] D.A. Evans, D.M. Barnes, J.S. Johnson, T. Lectka, P. von Matt, S.J. Miller, J.A. Murry, R.D. Norcross, E.A. Shaughnessy, K.R. Campos, J. Am. Chem. Soc. 121 (1999) 7582.
[12] D.A. Evans, J.S. Johnson, E.J. Olhava, J. Am. Chem. Soc. 122 (2000) 1635.
[13] J.M. Takacs, E.C. Lawson, M.J. Reno, M.A. Youngman, D.A. Quincy, Tetrahedron: Asymmetry 6 (1997) 3073.
[14] A.K. Ghosh, H. Cho, J. Cappiello, Tetrahedron: Asymmetry 9 (1998) 3687.
[15] J. Zhou, Y. Tang, Org. Biomol. Chem. 2 (2004) 429.
[16] A.K. Ghosh, P. Mathivanan, J. Cappiello, Tetrahedron: Asymmetry 9 (1998) 1.
[17] J.M. Fraile, J.I. García, M.A. Harmer, C.I. Herrerías, J.A. Mayoral, J. Mol. Catal. A Chem. 165 (2001) 211.
[18] P. O'Leary, N.P. Krosveld, K.P. De Jong, G. van Koten, R.J.M. Klein Gebbink, Tetrahedron Lett. 45 (2004) 3177.
[19] A. Corma, H. García, A. Moussaif, M.J. Sabater, R. Zniber, A. Redouane, Chem. Commun. (2002) 1058.
[20] R. Annunziata, M. Benaglia, M. Cinquini, F. Cozzi, M. Pitillo, J. Org. Chem. 66 (2001) 3160.
[21] K. Hallman, C. Moberg, Tetrahedron: Asymmetry 12 (2001) 1475.
[22] Y. Traa, D.M. Murphy, R.D. Farley, G.J. Hutchings, Phys. Chem. Chem. Phys. 3 (2001) 1073.
[23] S. Taylor, J. Gullick, P. McMorn, D. Bethell, P.C. Bulman Page, F.E. Hancock, F. King, G.J. Hutchings, J. Chem. Soc. Perkin Trans. 2 (2001) 1724.
[24] Y. Wan, P. McMorn, F.E. Hancock, G.J. Hutchings, Catal. Lett. 91 (2003) 145.
[25] D. Rechavi, M. Lemaire, J. Mol. Catal. A Chem. 182–183 (2002) 239.
[26] D. Rechavi, M. Lemaire, Org. Lett. 3 (2001) 2493.
[27] J.K. Park, S.-W. Kim, T. Hyeon, B.M. Kim, Tetrahedron: Asymmetry 12 (2001) 2931.
[28] M. Tada, T. Taniike, L.M. Kantam, Y. Iwasawa, Chem. Commun. (2004) 2542.
[29] M. Tada, N. Kojima, Y. Izumi, T. Taniike, Y. Iwasawa, J. Phys. Chem. B 109 (2005) 9905.
[30] M. Tada, Y. Iwasawa, Annu. Rev. Mater. Res. 35 (2005) 397.
[31] M. Tada, Y. Iwasawa, Chem. Commun. (2006) 2833.
[32] M. Tada, S. Tanaka, Y. Iwasawa, Chem. Lett. 34 (2005) 1362.
[33] D. Muller, G. Umbricht, B. Weber, A. Pfaltz, Helv. Chim. Acta 74 (1991) 232.
[34] S.E. Denmark, C.M. Stiff, J. Org. Chem. 65 (2000) 5875.
[35] E.A. Stern, M. Newville, B. Ravel, Y. Yacoby, D. Haskel, Physica B 208–209 (1995) 117.
[36] A.L. Ankudinov, B. Ravel, J. Rehr, S.D. Conradson, Phys. Rev. B 58 (1998) 7565.
[37] P. Ferreira, I.S. Gonçalves, F.E. Kühn, A.D. Lopes, M.A. Martins, M. Pillinger, A. Pina, J. Rocha, C.C. Romão, A.M. Santos, T.M. Satnos, A.A. Valente, Eur. J. Inorg. Chem. (2000) 2263.
[38] D. Muller, G. Umbricht, B. Weber, A. Pfaltz, Helv. Chim. Acta 74 (1991) 232.
[39] C. Bolm, M. Martin, G. Gescheidt, C. Palivan, D. Neshchadin, H. Bertagnolli, M. Feth, A. Schweiger, G. Mitrikas, J. Harmer, J. Am. Chem. Soc. (2003) 6222.
[40] G.G. Jernigan, G.A. Somorjai, J. Catal. 147 (1994) 567.
[41] B.J. Hathaway, D.E. Billing, Coord. Chem. Rev. 5 (1970) 143.
[42] M. Soibinet, I.D. Olivier, A. Mohamadou, M. Aplincourt, Inorg. Chem. Commun. 7 (2004) 405.
[43] M.H. Grootheaert, J.A. van Bokhoven, A.A. Battiston, B.M. Weckhuysen, R.A. Schoonheydt, J. Am. Chem. Soc. 125 (2003) 7629.
[44] L.S. Kau, D.J. Spira-Solomon, J.E. Penner-Hahn, K.O. Hodgson, E.I. Solomon, J. Am. Chem. Soc. 109 (1987) 6433.
[45] E.A. Stern, Phys. Rev. B 48 (1993) 9825.
[46] Y. Iwasawa (Ed.), Tailored Metal Catalysts, Reidel, Dordrecht, 1986.
[47] H. Wang, X. Liu, H. Xia, P. Liu, J. Gao, P. Ying, J. Xiao, C. Li, Tetrahedron 62 (2006) 1025.
[48] S.J. Bae, S.-W. Kim, T. Hyeon, B.M. Kim, Chem. Commun. (2000) 31.
[49] R. Hoen, J.A.F. Boogers, H. Bernsmann, A.J. Minnaard, A. Meetsma, T.D. Tiemersma-Wegman, A.H.M. de Vries, J.G. de Vries, B.L. Feringa, Angew. Chem. Int. Ed. 44 (2005) 4209.